JOINT INSTITUTE FOR NUCLEAR RESEARCH

Veksler and Baldin laboratory of High Energy Physics

FINAL REPORT ON THE START PROGRAMME

Analysis of Fixed Target Mode at MPD experiment: Track Efficiency

Supervisor:
Dr. Ivonne Alicia Maldonado Cervantes
Student:
Adrián Lara Tlaxcala.
Universidad Nacional Autónoma de México (UNAM)
Participation period:
June 30 – August 24, Summer Session 2024

August 23, 2024

Abstract

In this report we show an analysis of simulated data for the future fixed target experiment. 384,800 Events of $Xe^{124} + W$ at $T = 2.5$ GeV ($\sqrt{s_{AB}} = 2.9$ GeV) were simulated with the event generator UrQMD and analyzed with MpdRoot. Analysis on Primary Vertex, Track Reconstruction, Centrality and Track Efficiency were perform during the START program.

Contents

1 Introduction

1.1 Main Objective

The MPD experiment will start taking data in the fixed target configuration by mid−2025. Analysis on Fixed Target Xe^{124} + W at T = 2.5 GeV ($\sqrt{s_{AB}}$ = 2.9 GeV) is done on this report. Primary Vertex determination and Track Reconstruction optimization are the main objectives. For both goals, Track selection was used for optimization, selection on η (pseudorapidity), DCA (Distance of Closest Aproach) and Number of Hits were obtain. With those cuts we obtain Acepted Reconstructed Tracks from them Centrality Determination and Track Efficiency were done to visualize performace of TPC detector.

1.2 MPD

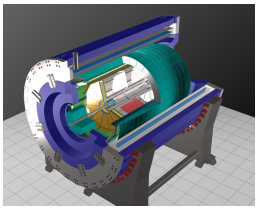

Figure 1: Image of simulated MPD detector

The Multi-Purpose Detector (MPD) is one of the two dedicated heavy-ion collision experiments of the Nuclotron based Ion Collider fAcility (NICA), one of the flagship projects, planned to come into operation at the Joint Institute for Nuclear Research (JINR) in April 2025. Its main objective is to search for new phenomena by colliding heavy nuclei in the energy range of 4 GeV $\leqslant \sqrt{s_{NN}} \leqslant$ 11 GeV. For these purposes the MPD has several key detectors. The central barrel components exhibit an approximate cylindrical symmetry within $|\eta| < 1.5$, comprising the Time Projection Chamber (TPC), the Time of Flight Detector (TOF), and the Electromagnetic Calorimeter (ECal). Additionally, the Fast Forward Detector (FFD) within the TPC barrel acts as a wake-up trigger, and the Forward Hadronic Calorimeter (FHCal) near the magnet end-caps helps determine collision centrality and the orientation of the reaction plane for collective flow studies.[1]

1.3 MpdRoot

Mpdroot is the off-line software framework for simulation , reconstruction and physics analyses of the simulated or experimental data for MPD experiment.[11].
MPDRoot is based on the Root environment (Data Analysis Framework) and the FairRoot framework, both built on an Object Oriented toolset in C++. Its main function is to facilitate transport through the detector and reconstruction of data, as detailed in fig. 2: Some of the event generators MPDRoot is able to analyze are:

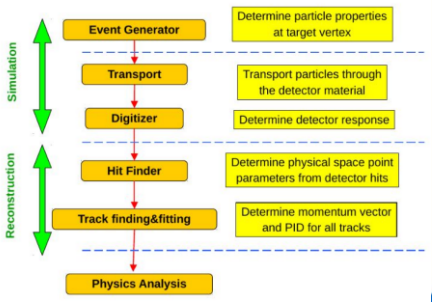

Figure 2: MpdRoot simulation and reconsruction procedure [6]

- Ultrarelativistic Quantum Molecular Dynamics (UrQMD)
- Quark-Gluon String Model (QGSM)
- Parton-Hadron-String Dynamics (PHSD)
- Pythia

In this study, UrQMD will be used as an event generator.

1.4 UrQMD

UrQMD (Ultra-relativistic Quantum Molecular Dynamics) is a computer simulation framework used in nuclear and particle physics to study the interactions of high-energy particles, particularly in heavy-ion collisions. It models the dynamics of the collision process from the initial stages of the collision, through the formation and evolution of a hot and dense medium (often referred to as a quark-gluon plasma), to the final stages where particles are emitted. It has a fully integrated Monte Carlo simulation package for Proton+Proton, Proton+nucleus and nucleus+nucleus interactions.

UrQMD employs concepts from quantum mechanics, statistical mechanics, and relativistic dynamics to simulate the complex interactions among quarks, gluons, and hadrons. Researchers use UrQMD to study various phenomena, including the properties of nuclear matter under extreme conditions, the dynamics of particle production in heavy-ion collisions, and the formation of exotic states of matter. [14]

1.5 Fixed Target Mode

Fixed-target experiments are those that study the collisions of a highly relativistic particle beam with a target that is stationary in the laboratory. This technique is complementary to collider experiments that study the collisions of particles from two opposed beams. [5]

In fixed target experiments, the energy available for interactions is determined by the energy of the incoming beam. In collider experiments, the collision energy is typically higher because it is determined by the combined energy of both colliding beams. The CM energy involved in a fixed target experiment rises as the square root of the incident energy $E_{cm} = \sqrt{2m_{2_0}E_{proj}}$. [10]

The fixed target experiments have a significant advantage for experiments that require higher luminosity (rate of interaction). [7]

The famous Rutherford gold foil experiment, performed between 1908 and 1913, was one of the first fixed-target experiments, in which the alpha particles were targeted at a thin gold foil. Nowdays there are successful fixed-target experimental programs such as NA49/NA61, HADES, BM@N here at JINR, Fermilab [8] and others.

1.6 Centrality

Centrality is a quantity crucial on collision of heavy-ion, because it measures the overlap region between the two nuclei in a collision. This quantity is characterised by the impact parameter (b) between the two nuclei, i.e. the distance between their centres in the plane transverse to the beam axis. The impact parameter defines the overlap region of the nuclei and thus determines also the size and shape of the resulting medium. A schematic view of a heavy-ion collision is shown in Fig. 3. The geometry of the collision is related to the number of nucleons that participate in it and the number of nucleon-nucleon collisions. These quantities are not directly accessible and hence need to be derived from the data recorded during the collisions by making use of other quantities that scale approximately with the number of participating nucleons, such as the outgoing particle multiplicity. For this purpose, a Glauber model is often used. [4]

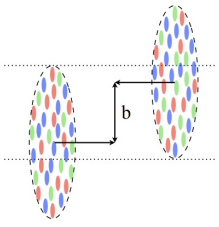

Figure 3: A schematic view of a heavy-ion collision. The impact parameter b is shown as well

1.6.1 Glauber

Glauber method is a computational method that performs centrality determination using multiplicity distribution at mid rapidity. The way in that MC Glauber method determinates centrality is using the following formula:

$$c_{N_{ch}} = \frac{1}{\sigma_{inel}} \int_{N_{ch}}^{\infty} \frac{d\sigma}{dN_{ch}} dN_{ch} \tag{1}$$

where:
σ_{inel} - Inelastic cross section,
N_{ch} - Multiplicity of charge particles,
$\frac{d\sigma}{dN_{ch}}$ - Probability of an inelastic collision for a given N_{ch}.
The Glauber model calculation is performed in two steps. First, the nucleon position in each nucleus are stochastically determined. Then, the two nuclei are collided, asumming the nucleons travel in a straight line along the beam axis and the nucleons move independenly inside of the nucleus.

1.6.1.1 First Step The nucleon density inside the nucleus is provided as an input of the Glauber model [9]. This density can be described by the Fermi (or modified Woods-Saxon) distribution:

$$\rho(r) = \rho_0 \frac{1 + w\left(\frac{r}{R}\right)^2}{1 + exp\left(\frac{r-R}{a}\right)} \tag{2}$$

where:
R - Radius of the nucleus
ρ_0 - density at the center of the nucleus
a - skin thickness of the nucleus
w - describe when the maximum density is reached

1.6.1.2 Second Step The second step is simulate a nuclear collision. The nucleus-nucleus collision is treated as a sequence of independent binary nucleon-nucleon collisions, where the nucleons travel on straight line trajectories and the inelastic nucleon-nucleon cross section is assumed to be independent of the number of collisions a nucleon underwent previously. With that assumsions two nucleons collide if the relative transverse distance between centers is less than the distance corresponding to the inelastic nucleon-nucleon cross section:

$$d < \sqrt{\frac{\sigma_{NN}^{inel}}{\pi}}$$

Inelastic cross section is given as an input.

1.6.1.3 Obtaintion of N_{part} and N_{coll}

Glauber method output N_{part} and N_{coll} using the following formulas:

$$N_{coll}(b) = \sum_{n=1}^{AB} nP(n,b) \tag{3}$$

$$N_{part} = A \int \hat{T}_A(\vec{s})\{1-[1-\hat{T}_B(\vec{s}-\vec{b})\sigma_{inel}^{NN}]^B\}d^2s + B \int \hat{T}_B(\vec{s}-\vec{b})\{1-[1-\hat{T}_A(\vec{s})\sigma_{inel}^{NN}]^B\}d^2s \quad (4)$$

Where: $\hat{T}_i(\vec{s})$ is the Thickness function and $P(n,\vec{b})$ is a binomal distribution for the probability of having n interactions between nucleus A and B. This two expresions are defined and explain on ref. [9] in page 9.

2 Event generation for Fixed Target Mode Configuration

For our analysis, we simulate 384,800 $Xe^{124} + W$ collisions at $T = 2.5$ GeV using UrQMD as a Monte Carlo Event Generator with the following input: [14]

```
pro 124 54          //Proyectile Atomic_mass Atomic_number
tar 184 74          //Target Atomic_mass Atomic_number

nev 200             //Number of Events
imp -14.71          //Impact Parameter
ene 2.5             //Kinetic Energy
tim 200 200         //Time

cto 27 1            //Target Mode Option

rsd 16537010        //Random Number
f13
#f14                //Output File
f15
f16
f19
f20

xxx
```

We configure the script runMC.C for Fixed Target (FXT), positioning the target at -85 cm and no smearing of vertex, on code we set the variables as appears in the following box:

```
primGen->SetBeam(0.0, 0.0, 1e-6, 1e-6);
primGen->SetTarget(-85.0, 0.0);
primGen->SmearGausVertexZ(kFALSE);
primGen->SmearVertexXY(kFALSE);
```

Finally we process the events with the runReco.C script to obtain the mpddst.root files. The mpddst.root files contain all the information about event and the reconstructed tracks.

3 Primary Vertex Analysis

As a first step we analyze the distribution of the z coordinate of the reconstructed primary vertex, shown in Figure 1.

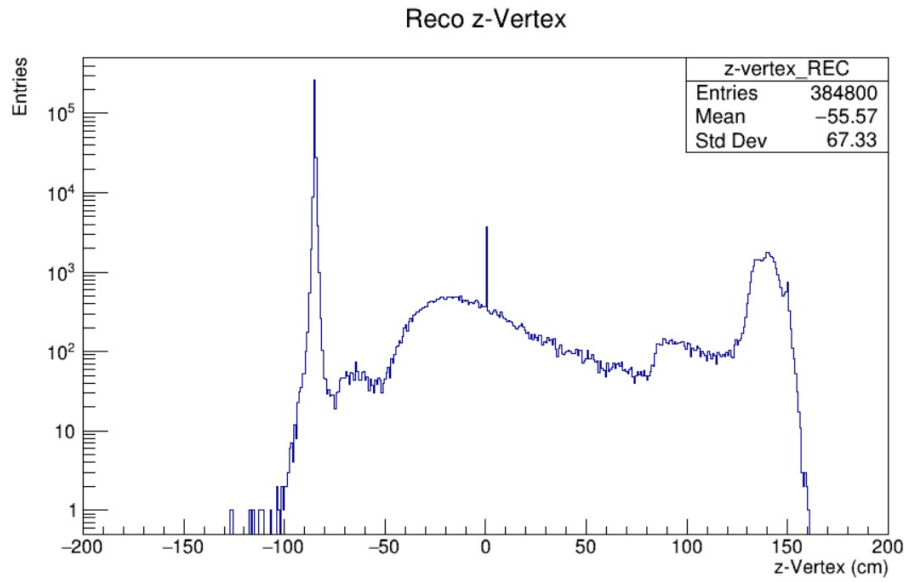

Figure 4: Distribution of z-coordinate of reconstructed primary vertex

The distribution has a peak at $z_{Vertex} = -85.0$ cm, however there are several events in the range -50 cm to 150 cm. To estimate the contribution of the events in this region, we calculate the percentage of events around the -85 cm peak. The percentage of events with $z_{vertex} \in (-100, -70)$ cm its 80.164% of the total events. To reject this events we apply a cut to the number of MCTracks from each event, for the analysis we select events with more than 308 tracks (124 from Xenon and 184 from Wolfram), so we ensure events with more particles than the initial ones. The distribution obtained is shown on Figure 5.

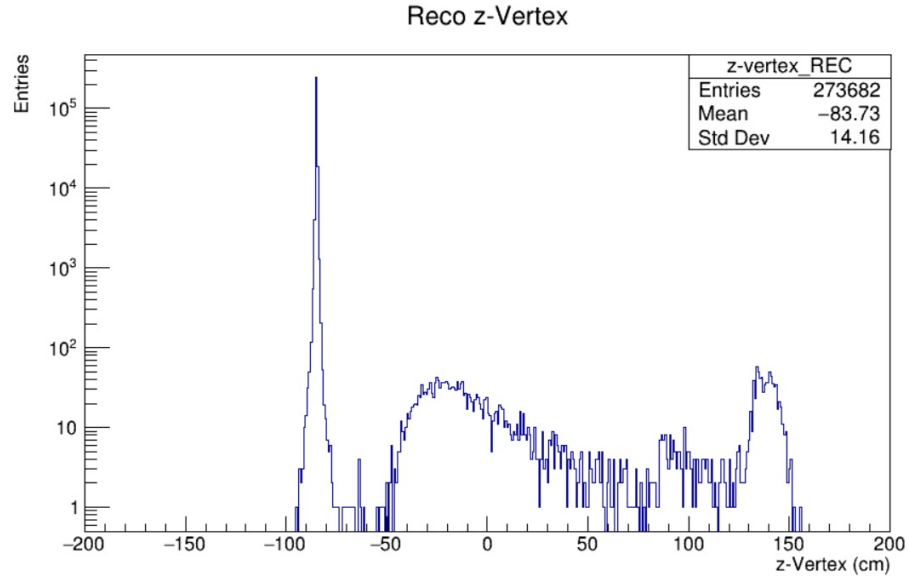

Figure 5: Primary z-Vertex distribution with number of MCTracks higher than 308.

Again we calculate the percentage of events around the -85 cm peak and now it is 98.95% of the total events. We can conclude that contribution of events on $z_{vertex} \in (-50, 150)$ cm its not relevant and can be ignored. Most of the rejected events correspond to peripheral events, as we can see in the distribution of the impact parameter in figure 6.

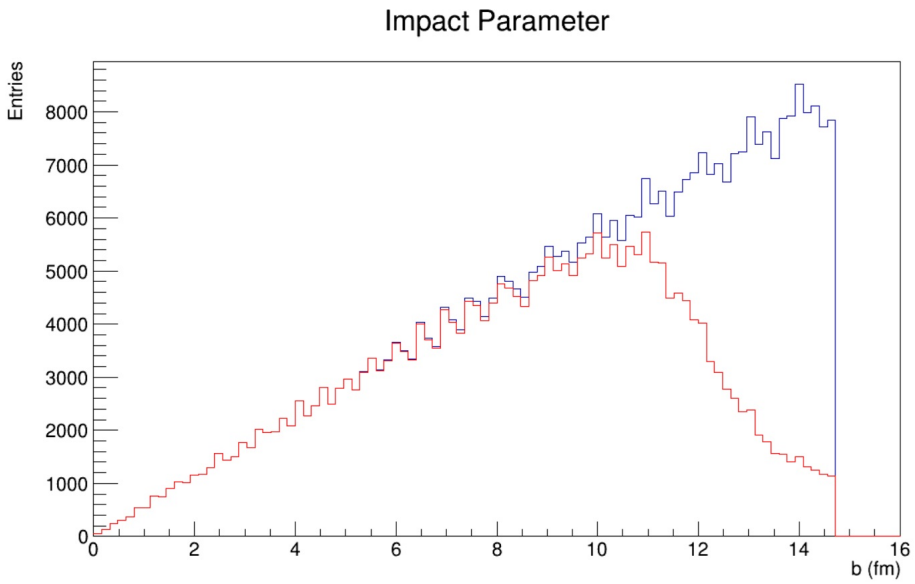

Figure 6: Distribution of the Impact parameter of the events without (blue) cut on the number of MCTracks and with cut (red) on MCTracks > 308.

On peripheral collisions multiplicity produced is low, so the primary vertex reconstruction is not good as we can check from fig.7, where resolution on primary vertex

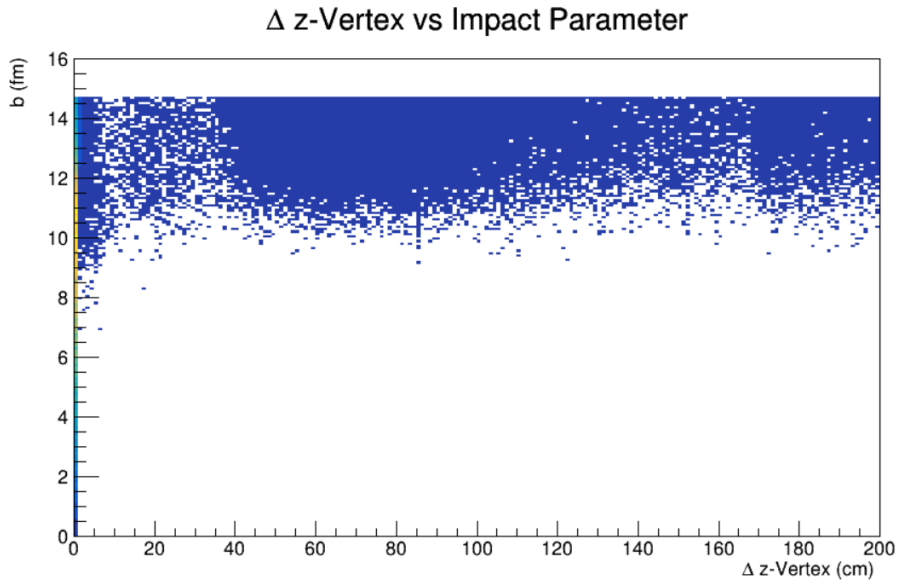

Figure 7: Distribution of z-Vertex Resolution vs Impact parameter

4 Reconstructed Track selection

To select the tracks, we analyze the transverse momentum resolution

$$\delta p_T = \frac{\left|p_T^{Reco} - p_T^{MC}\right|}{p_T^{MC}} \tag{5}$$

as a function of different variables used to select good reconstructed tracks, as the number of hits in the TPC (Time Projection Chamber), the pseudorapidity η and the DCA (Distance of

Closest Approach). The distribution of δp_T is shown in the figures 9 and 10 for primary and secondary particles respectively. To parametrize aceptance on reconstructed tracks we select tracks with $\delta p_T < 0.2$. Also, we need to clarify that we are using a cut on $z_{vertex} \in (-100, -70)$ cm to restric our view to peak at $z_{vertex} = -85$ cm and a cut on impact parameter $b < 13$ to eliminate even more peripheral events.

First, phase space of pseudorapidity and p_T is shown on fig.9, with this distribution we will observe in detail how cuts will clean the distribution.

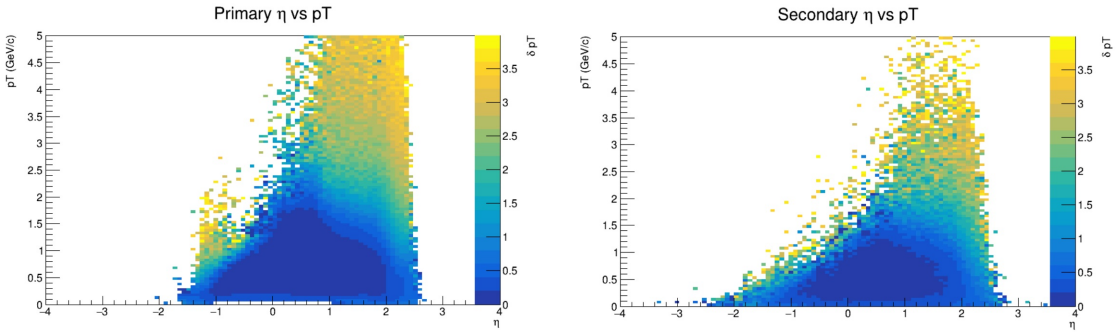

(a) Phase space for primary particles (b) Phase space for secondary particles

Figure 8: Phase space η vs p_T distributions with no cuts on reconstructed tracks (δp_T is on palette)

TProfile were made for primary particles on fig. 9 and secondary particles on fig.10 that gives an average of values with respect to p_T resolution. Limit on $\delta p_T < 0.2$ is delimited by a red line on histograms.

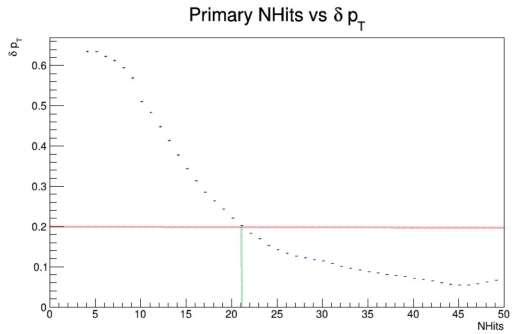

(a) Number of Hits vs p_T Resolution for Primary Particles.

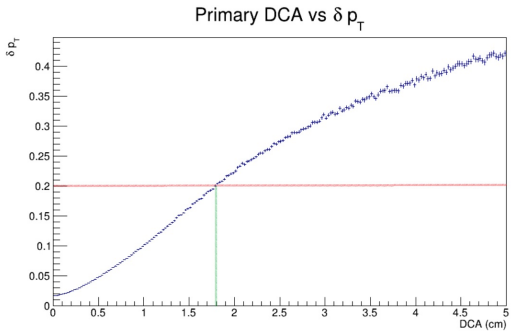

(b) DCA vs p_T Resolution for Primary Particles.

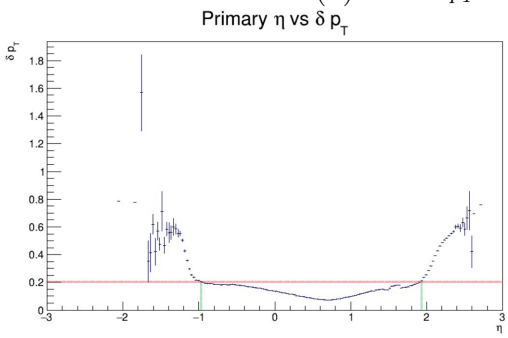

(c) η vs p_T Resolution for Primary Particles.

Figure 9: Primary Particles selected with MC association.

For primary particles the cuts taken are: Number of hits at 20, DCA at 1.7 cm and $\eta \in [-1, 2]$.

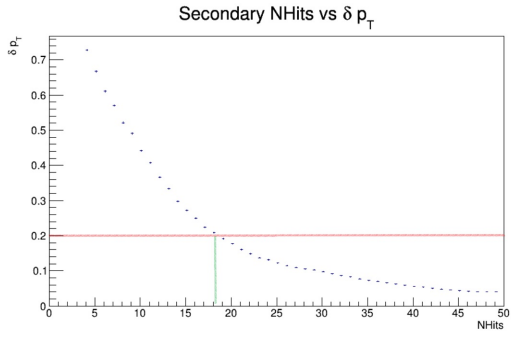

(a) Number of Hits vs p_T Resolution for Secondary Particles.

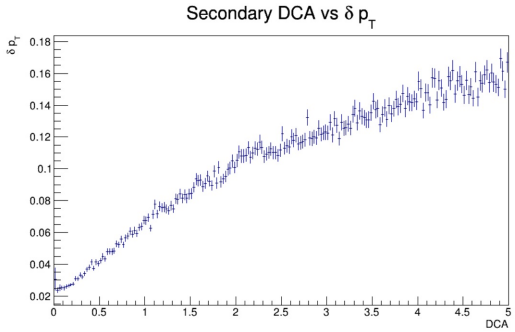

(b) DCA vs p_T Resolution for Secondary Particles.

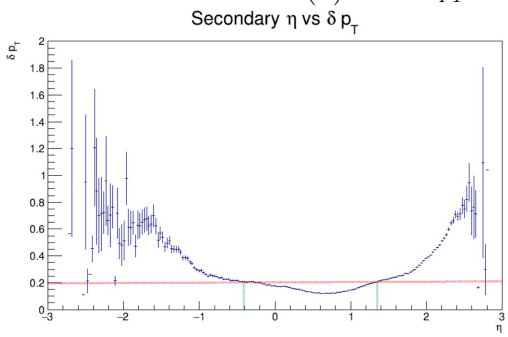

(c) η vs p_T Resolution for Secondary Particles.

Figure 10: Secondary Particles selected with MC association.

For secondary particles the cuts taken are: Number of hits at 17 and $\eta \in [-0.2, 1.2]$.On DCA distribution for secondary particles, all of them have resolution of p_T less than 0.2, so we are going to take a cut where $\delta p_T < 0.1$, and we get DCA = 2 cm.
All of this restrictions have to be applied to a track, so we will take global restriction as follows:

Variables	Cut for Accepted Tracks
Number of Hits	Nhits $\geq$ 20
DCA	DCA $\leq$ 2 cm
Pseudorapidity	$\eta \in [-1, 2]$

Table 1: Restrictions for Accepted Tracks

Now that we obtain the cuts, we can remake the phase space distribution as shown on fig.11

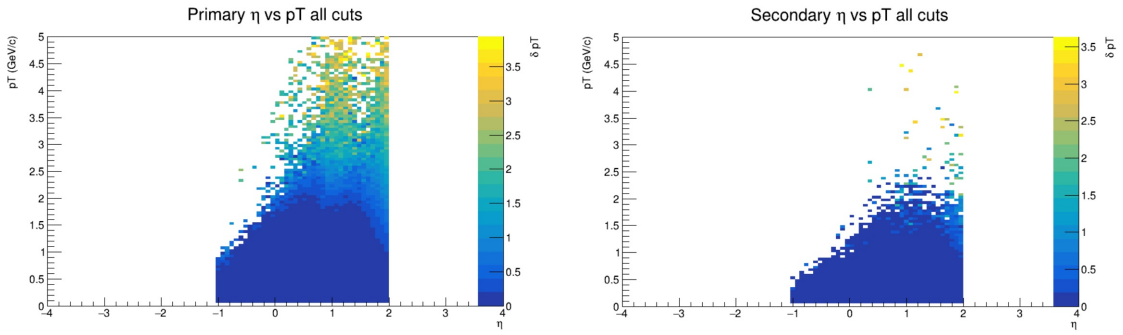

(a) With cuts on $\eta \in [-1, 2]$, $DCA \leq 2$ cm , $NHits \geq 20$

(b) With cuts on $\eta \in [-1, 2]$, $DCA \leq 2$ cm , $NHits \geq 20$

Figure 11: Phase space η vs p_T distributions with accepted reconstructed tracks (δp_T is on palette)

We observe that for primary particles on fig.11a the p_T resolution is too big for particles with $p_T > 2$ GeV/c. Same for secondary particles on fig.11b.
Also from fig.11 we can observe that phase space is not symmetric with respect to pseudorapidity, this is because for values $\eta < 0$, p_T values had a maximum at 1 GeV/c.

Now with conditions of Accepted Reconsructed Tracks, Multiplicity distribution shown in figure 16 was made for Centrality Determination.

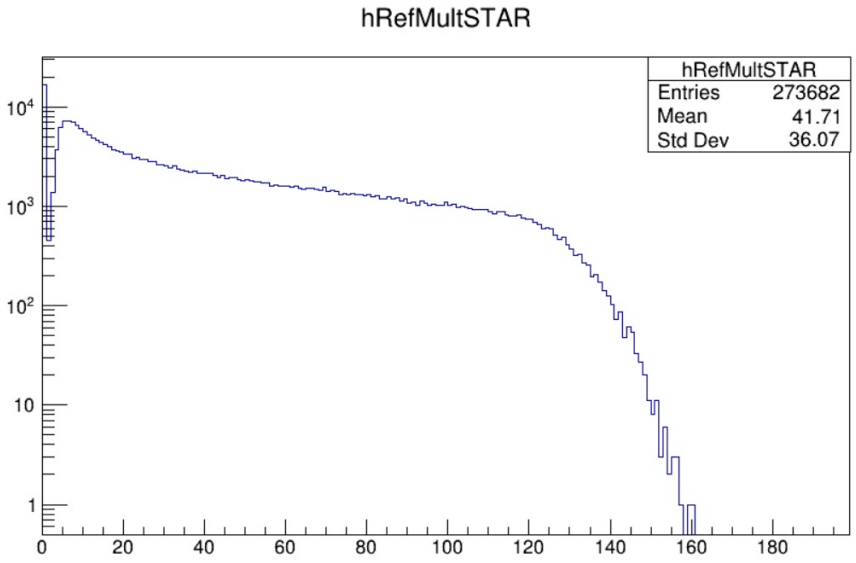

Figure 12: Multiplicity distribution cuts on b, Number of Hits, DCA and η.

5 Centrality Determination using MC Glauber

5.1 MC Glauber Procedure

For MC Glauber method it is needed:

- The nucleon nucleon inelastic cross section σ_{NN}.
- Multiplicity distribution.

Formula and procedure to obtain inelastic cross section are in the appendix. From the calculation we obtain a result of $\sigma_{inel} = 26.94035$ mb. Inelastic cross section depends on the energy of the collision and their values are parametrized for different energy, unfortunately there is no unique parametrization for low energies, which is our case, more information about our parametrization is on apendix and ref. [2]

5.1.1 Implementation of MCGlauber

To obtain Centrality we follow the instruction on the Centrality Framework [3], on this website it is explain how to use MC Glauber method that uses Glauber. Here we going to explain it briefly.
Glauber makes a simulation of collision of two heavy-ion, then all of this data is pass to the Centrality Framework, which performs a fitting procedure using a negative binomial distribution process with different parameters. Then it begins to look for the best error, finally Centrality Framework divide the fitting by centrality classes. A graphic summary is on Figure. 13. More explanition is on Github [13], where it can be found a document explaining MCGlauber and Gamma Fit procedure.

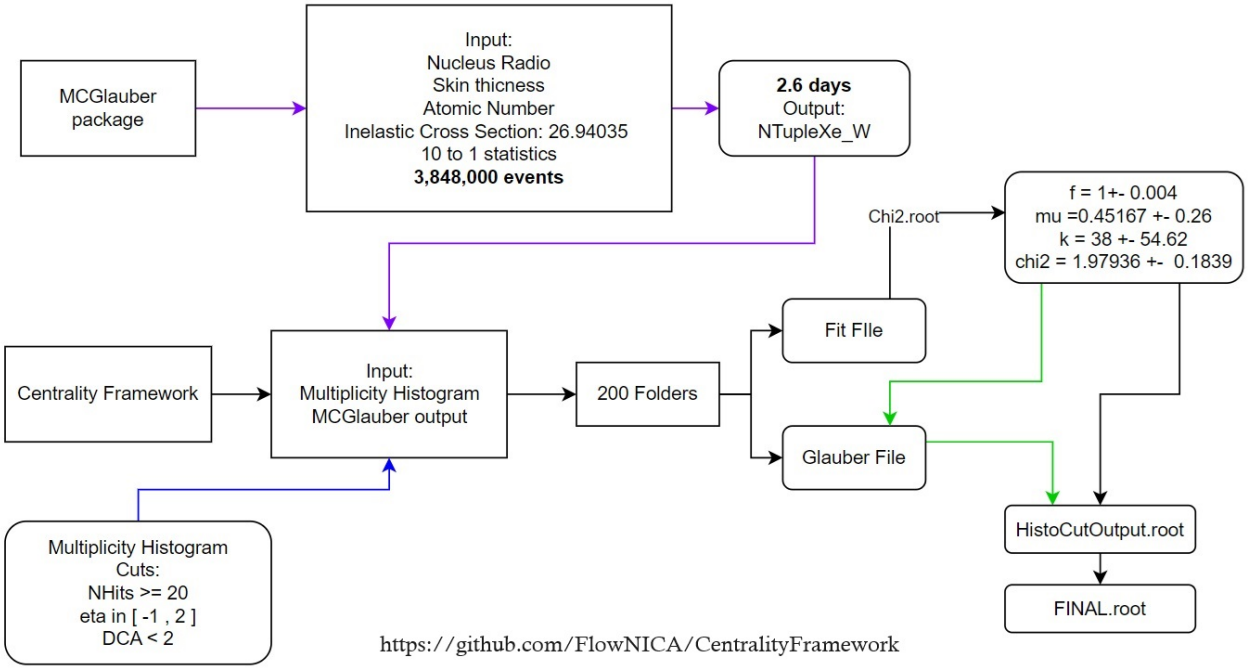

Figure 13: Graphic Summary of the MC Glauber procedure

5.2 MCGlauber results

All results from MC Glauber

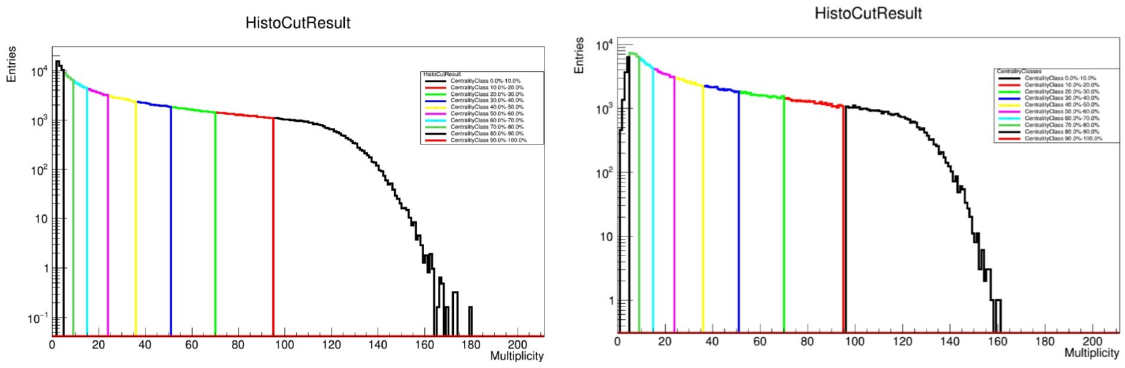

(a) Multiplicity fitted function (b) Multiplicity input ditribution

Figure 14: Multiplicity ditribution divided by centrality Classes

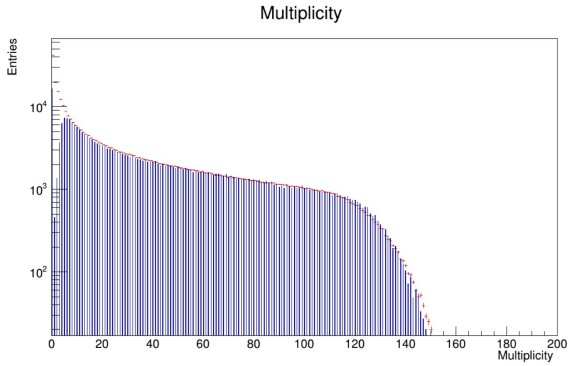

Figure 15: Multiplicity Distribution, on blue input distribution, on red fitted distribution

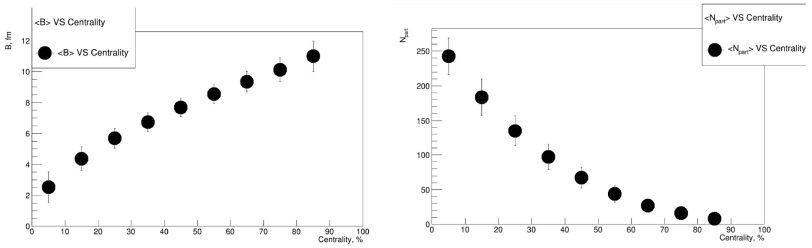

(a) Mean impact parameter vs Centrality (b) Mean Number of participants vs Centrality

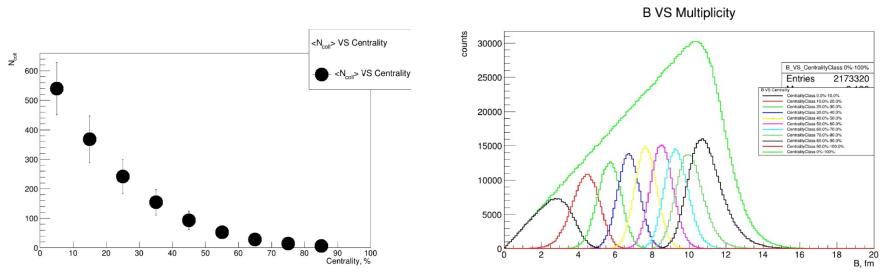

(c) Mean Number of collision vs Centrality (d) Impact parameter divided by centrality Classes

Figure 16: Histograms divided by Centrality Classes

Table of N_{part}, N_{coll}, mean N_{part}, N_{coll} and mean impact parameter for each centrality class.

Centrality, %	N_{ch}^{min}	N_{ch}^{max}	$\langle b \rangle$, fm	RMS	$\langle N_{part} \rangle$	RMS	$\langle N_{coll} \rangle$	RMS
0 - 10	95	164	2.54	1.00	242.75	26.44	539.73	88.76
10 - 20	70	95	4.37	0.76	183.50	26.19	367.84	79.38
20 - 30	51	70	5.69	0.63	134.96	21.54	241.37	59.12
30 - 40	36	51	6.74	0.59	97.33	17.96	154.42	43.75
40 - 50	24	36	7.68	0.59	67.38	14.84	93.66	31.25
50 - 60	15	24	8.55	0.61	43.96	11.82	52.81	20.86
60 - 70	9	15	9.35	0.66	27.27	9.01	28.33	13.12
70 - 80	5	9	10.11	0.78	16.04	6.73	14.59	8.12
80 - 90	2	5	10.99	0.99	8.23	4.74	6.60	4.77

Table 2: Results table of MC Glauber method

5.3 Comparation with Gamma Fit

The determination of centrality was a joint work with my colleague Francisco Reyes from the START Program, from which data were obtained and compared ref. [12], this data was performed with an alternate method to the MC Glauber called Gamma Fit.

Centrality, %	$N_{chMCGlauber}^{min}$	$N_{chMCGlauber}^{max}$	$N_{chGammaFit}^{min}$	$N_{chGammaFit}^{max}$	ΔN_{ch}^{min}	ΔN_{ch}^{max}
[0 - 10]	95	164	96	162	1	2
[10 - 20]	70	95	70	96	0	1
[20 - 30]	51	70	50	70	1	0
[30 - 40]	36	51	34	50	2	1
[40 - 50]	24	36	33	34	9	2
[50 - 60]	15	24	15	23	0	1
[60 - 70]	9	15	9	15	0	0
[70 - 80]	5	9	5	9	0	0
[80 - 90]	2	5	1	5	1	0

Table 3: Multiplicities extracted with the MC Glauber and Gamma Fit method and difference between them divided by centrality classes [12]

From table.3 we can observe multiplicity of charge particles for both methods, making the diferences between multiplicities we can see that there is almost no difference between methods, so for our analysis we can use either of them. Same for average impact parameter on fig.17 where is shown the relation between them.

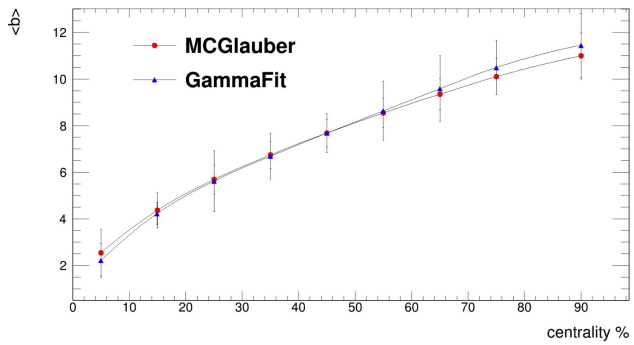

Figure 17: Average impact parameter comparison between MC Glauber and Gamma Fit method

6 Tracking Efficiency

Track efficiency is define as the ratio between Accepted Reconstracted Tracks over Monte-Carlo Tracks:

$$Eff = \frac{p_T^{Reco}}{p_T^{MC}} \tag{6}$$

On this project, track efficiency is done by primary and secondary particles and by particle species, Protons, Kaons, Pions. This procedure is used to evaluate detector performance on particle detection, we need to emphasize that the calculated efficiency its done with MonteCarlo Identification. Using Particle Identification was made by my partner Franscisco Reyes on his report titled as "Analysis of Fixed Target Mode at MPD experiment: Particle identification" on ref. [12]

6.1 Track Selection

For Accepted Reconstracted Tracks, it was explain on previous sections. For MC Tracks, track selection was made mathching cuts made on Reconstructed Tracks, but not all cuts can be translated to MC Tracks. The cuts made were:

Cut for Accepted Tracks	Cut for Accepted Tracks
Nhits ≥ 20	$z_{vertex} \in (-100, -70)$ cm
DCA ≤ 2 cm	Impact parameter b <13
$\eta \in [-1, 2]$	$\eta \in [-1, 2]$
$z_{vertex} \in (-100, -70)$ cm	
Impact parameter b <13	

Table 4: Cuts made for Accepted Tracks and MonteCarlo Tracks

6.2 Track Efficiency with respect to p_T

With this selection, division of p_T Histograms were made to obtain efficiency:

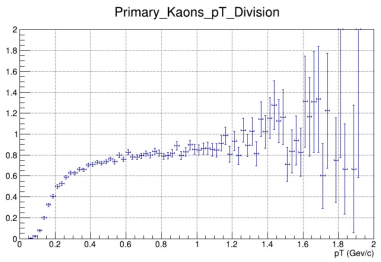

(a) Track Efficiency for Primary Kaons

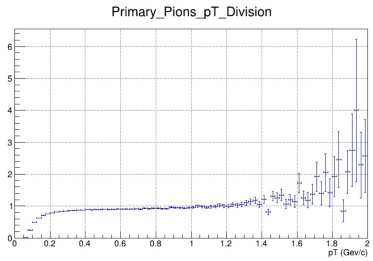

(b) Track Efficiency for Primary Pions

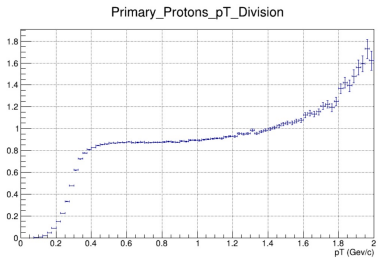

(c) Track Efficiency for Primary Protons

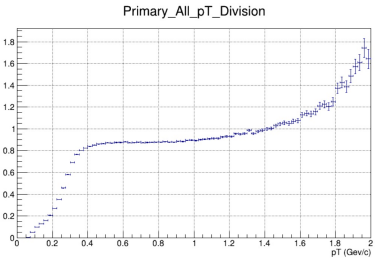

(d) Track Efficiency for All Primary Particles

Figure 18: Track Efficiency for Primary Particles using MonteCarlo Asosiation

From above distributions on fig.18, track efficiency for all primary particles stays below 1 til $p_T = 1.4$ GeV/c. For greater values of p_T, track reconstruction is not correct. This pattern is present in protons as well. For Pions and Kaons, efficiency stays below 1 til about $p_T = 1.2$ GeV/c. This p_T values can be explain by transversal momentum resolution with p_T on fig.19 it is shown that p_T has a resolution lower than 20% when p_T values are below 1.2 GeV/c, from that we can conclude that for best tracking reconstruction a cut on $p_T < 1.2$ GeV/c can be done.

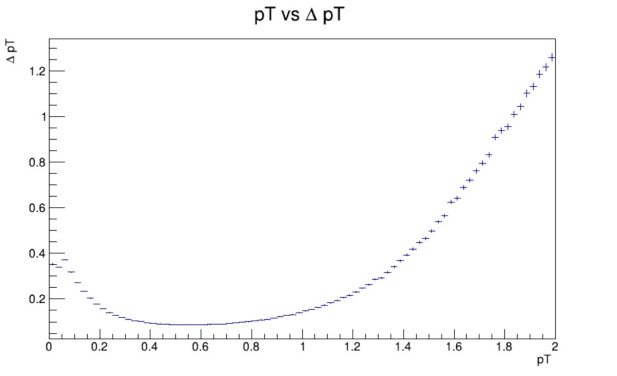

Figure 19: Distribution of Transversal momentum vs Resolution of transversal momemtum

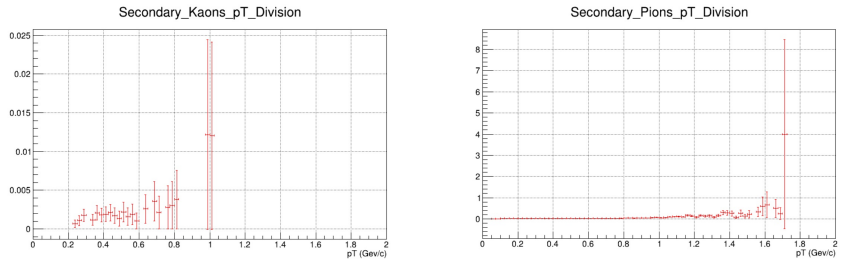

(a) Track Efficiency for Secondary Kaons

(b) Track Efficiency for Secondary Pions

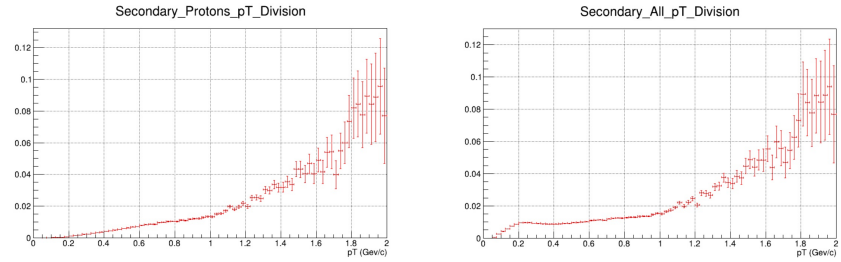

(c) Track Efficiency for Secondary Protons

(d) Track Efficiency for All Secondary Particles

Figure 20: Track Efficiency for Secondary Particles using MonteCarlo Asosiation

From Figure 20, we can observe that efficiency is not done correctly, because it should have a similar behaviour as the efficiency for primary particles. One of the reasons to explain this behaviour is on Fig. 21, in which we show the starting position where secondary particles are being created, this is obtain through MC Tracks, with this we can observe that most of the secondary particles are on the edges of the detector, so reconstruction its not well done or particles don't collide with the detector, and therefore we don't obtain enough reconstructed Tracks.

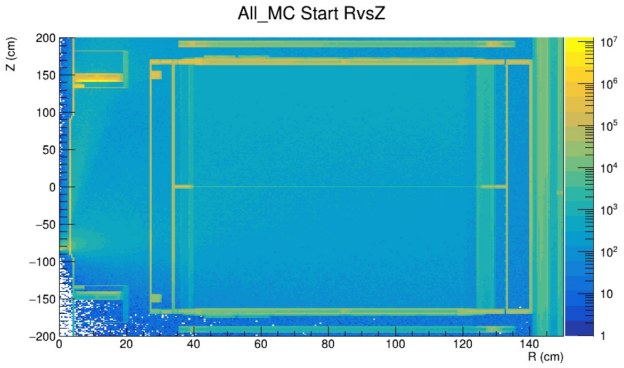

Figure 21: Histogram of initial position of Secondary particles

One of the ways this could be fixed is by making a restriction on MC Tracks discarding tracks with not enough time of flight on the TPC. Fixing efficiencies couldn't be completed on the time for the START program, it will be done on later works.

6.3 Track Efficiency with respect to η and z-Vertex

Track efficiency was also perform with respect to η and z-Vertex.

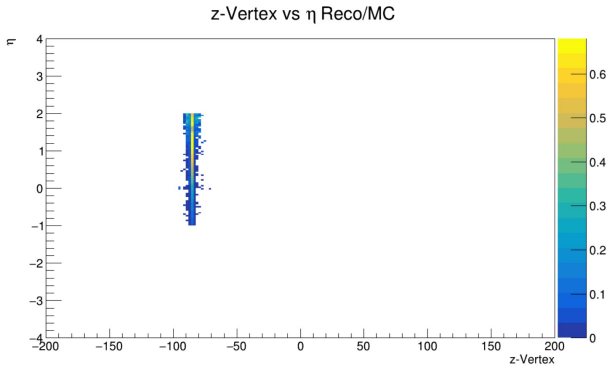

Figure 22: Track Efficiency Histogram of η vs z-Vertex

With this distribution we can perform a identification of centrality per event using centrality wagon of MpdRoot, that procedure couldn't be done on time of START program.

7 Summary

We detail the Analysis on Fixed Target experiment of $Xe^{124} + W$ at $T = 2.5$ GeV, using simulated data generated with UrQMD. On this analysis we obtain a region on Primary Vertex where most events generate more particles than the initial ones.
Using that restriction, we select Reconstructed Tracks using the resolution of p_T less than 0.2 as a reference for acceptance of Tracks. Thereby obtaining cuts in Number of Hits on TPC, pseudorapidity and DCA.
We use them to obtain a multiplicity distribution, which was needed to determinate centrality using MC Glauber method. Also using this cuts, Tracking Efficiency was done to observe performance on TPC at Track Reconstruction.
All of the work done on START Program will be continue later on. Planned future work is to finish centrality identification by species of particles using particle identification.

8 Acknowledgement

I would like to express my sincere thanks to my supervisors, Dr. Vadim Kolesnikov, Dr. Ivonne Maldonado, Dr. Viktar Kireyeu and Natalia Kolomoyets, for their support and guidance during my work on START. Thank you especially for your willingness to answer my questions with that guide I managed to overcome the obstacles presented. It is a pleasure to have had the opportunity to work with them and I hope to continue counting with their support.

9 Appendix

9.1 Inelastic Cross Section

To obtain the inelastic cross section we used the following formula:

$$\sigma_{inel} = \sigma_{total} - \sigma_{ela} \tag{7}$$

where:

- σ_{total} - Total cross section
- σ_{ela} - Elastic cross section
- σ_{inel} - Inelastic cross section

Total and Elastic cross Section were obtain on ref. [2] in page 116, the range of energy on which following formulas have meaning its at $\sqrt{s} > 2.6$ GeV:

$$\sigma_{total} = 48.0 + 0.522ln^2(p_{lab}) - 4.51ln(p_{lab}) \tag{8}$$
$$\sigma_{ela} = 11.9 + 26.9p_{lab}^{-1.21} + 0.169ln^2(p_{lab}) - 1.85ln(p_{lab}) \tag{9}$$

where: p_{lab} - momentum in the lab [Gev/c]
The momentum in the lab needs to be calculated. Our experiment is a Fixed Target experiment at $T = 2.5$ GeV ($\sqrt{s} = 2.9$ GeV).
So our p_{lab} has to be the momentum of the projectile.

$$T = E_{proy} - E_0$$
$$E_{proy} = T + E_0 = 2.5 + 0.938 = 3.438$$
$$E_{proy}^2 = m^2 + p_{lab}^2$$
$$p_{lab} = \sqrt{E_{proy}^2 - m^2} = 3.3075$$

From the calculation we obtain a result of $\sigma_{inel} = 26.94035$ mb.

Bibliography

[1] Vahagn Abgaryan et al. "Status and initial physics performance studies of the MPD experiment at NICA". In: *The European Physical Journal A* 58.7 (2022), p. 140.

[2] O. Buss et al. "Transport-theoretical description of nuclear reactions". In: *Physics Reports* 512.1–2 (Mar. 2012), pp. 1–124. ISSN: 0370-1573. DOI: 10.1016/j.physrep.2011.12.001. URL: http://dx.doi.org/10.1016/j.physrep.2011.12.001.

[3] Peter Parfenov. *Centrality Framework*. URL: https://github.com/FlowNICA/CentralityFramework/.

[4] LHCb collaboration. *Centrality determination in heavy-ion collisions with the LHCb detector*. 2021. arXiv: 2111.01607 [nucl-ex]. URL: https://arxiv.org/abs/2111.01607.

[5] *Detectors, Fixed-Target — Encyclopedia.com*. URL: https://www.encyclopedia.com/science/encyclopedias-almanacs-transcripts-and-maps/detectors-fixed-target.

[6] *First Computing Workshop for interested students at MPD experiment*. Feb. 2024. URL: https://indico.jinr.ru/event/4393/.

[7] *fixed*. URL: https://ed.fnal.gov/painless/htmls/fixed.html.

[8] Gaston Gutierrez and Marco A. Reyes. "Fixed target experiments at the Fermilab Tevatron". In: *International Journal of Modern Physics A* 29.28 (Nov. 2014), p. 1446008. ISSN: 1793-656X. DOI: 10.1142/s0217751x14460087. URL: http://dx.doi.org/10.1142/S0217751X14460087.

[9] Michael L. Miller et al. "Glauber Modeling in High-Energy Nuclear Collisions". In: *Annual Review of Nuclear and Particle Science* 57.1 (Nov. 2007), pp. 205–243. ISSN: 1545-4134. DOI: 10.1146/annurev.nucl.57.090506.123020. URL: http://dx.doi.org/10.1146/annurev.nucl.57.090506.123020.

[10] Raghunath Sahoo. *Relativistic Kinematics*. 2016. arXiv: 1604.02651 [nucl-ex]. URL: https://arxiv.org/abs/1604.02651.

[11] *Simulation and Analysis Framework for the MPD experiment of the NICA project*. URL: https://mpdroot.jinr.ru/.

[12] *START - STudent Advanced Research Training at JINR*. Aug. 2024. URL: https://students.jinr.ru/?archive_reports.

[13] START STUDENTS. *IAMALDONADO/start$_s$ummer*24. Aug. 2024. URL: https://github.com/iamaldonado/START_Summer24.

[14] *URQMD / FIAS*. URL: https://urqmd.org/.